The role of the dielectric barrier in narrow biological channels: a novel composite approach to modeling single channel currents.

Artem Mamonov[*], Rob D. Coalson[*], Abraham Nitzan[#], and Maria G. Kurnikova[§†]

[*] Chemistry Department, University of Pittsburgh, Pittsburgh, PA 15260, USA. [#] School of Chemistry, University of Tel Aviv, Israel. [§] Chemistry Department, Marquette University, Milwaukee, WI 53202, USA.

Abstract

Ion currents through the Gramicidin A channel are modeled and compared to experimental results. The proposed approach utilizes a modified version of Poisson-Nernst-Planck (PNP) theory, termed Potential of-Mean-Force-Poisson-Nernst-Planck (PMFPNP) theory, to compute ion currents. As in standard PNP, ion permeation is modeled as a continuum drift-diffusion process in a self-consistent electrostatic potential. In PMFPNP, however, the free energy of inserting a single ion into the channel i.e., the potential of mean force (PMF) along the permeation pathway, is calculated using a combined molecular/continuum method using equilibrium molecular dynamics (MD) simulations of ions in the channel to sample dynamic protein configurations. Therefore, the dynamic flexibility of the channel environment is accounted for via the PMFPNP prescription. This approach reveals that equilibrium fluctuations of the channel molecule result in significant electrostatic stabilization of an ion inside the channel. The dielectric-self energy of the ion remains essentially unchanged in the course of the MD simulation, indicating that no substantial changes in the protein geometry occur as the ion passed through it. The diffusion coefficient of a potassium ion within the channel is also calculated using the MD trajectory. Therefore, no direct fitting parameters are required in our model. This model accounts for the experimentally observed saturation of ion current with increase of the electrolyte concentration, in contrast to the predictions of standard PNP theory.

1 Introduction

Ion permeation through narrow protein channels is a topic of considerable current interest (Andersen and Koeppell, 1992;Eisenberg, 1999;Hille et al., 1999;Roux et al., 2000;Kuyucak et al., 2001). The importance of ion transport for many vital cell functions is difficult to overestimate. Processes in which substantial ionic currents are generated in membrane channels include maintenance of ionic concentration gradients across the cell membrane, generation of action potentials in neurons and auto-waves in heart muscle to name just three. Moreover, many modern drugs target ionic channels to modify their action (Nilius and Droogmans, 2001;Lerche et al., 2001;Antonov, 2001;Marban, 2002). Therefore, in addition to extensive experimental effort, there

[†] Corresponding author. email: maria.kurnikova@marquette.edu

is much theoretical interest in understanding mechanisms of ion channel function at the molecular level. Recent advances in solving 3D structures of membrane proteins in general and channel proteins in particular (Koprowski and Kubalski, 2001) have enabled attempts at detailed molecular level modeling of ion current through protein channels (Kurnikova et al., 1999;Allen et al., 1999;Chung et al., 1999;Cardenas et al., 2000;Roux et al., 2000) (see also recent reviews of the subject (Kuyucak et al., 2001;Tieleman et al., 2001)). A first attempt to perform a full scale non-equilibrium Molecular Dynamics (MD) simulation of ion current through a simplified model channel at very high ion concentrations and applied voltage has been reported recently (Crozier et al., 2001). However, non-equilibrium MD simulations are too expensive for realistic biological ion channel systems at physiological conditions because of the many different time-scales and length-scales involved. Instead, several Dynamic Monte-Carlo (DMC) (Graf et al., 2000;Graf et al., 2002) and Brownian Dynamics (BD) studies (Corry et al., 2001;Chung et al., 1999;Allen et al., 1999;Im et al., 2000;Burykin et al., 2002;Mashl et al., 2001) of current-voltage relations through different natural and model channels have been recently reported. A key conclusion drawn from these studies is that the dielectric self-energy (DSE) (Graf et al., 2000;Schuss et al., 2001;Graf et al., 2002) which arises when an ion moves through a relatively narrow channel with diameter of up to ca.1 nm greatly affects the dynamics of ion permeation (Allen et al., 1999;Corry et al., 2000;Graf et al., 2000;Graf et al., 2002;Dieckmann et al., 1999;Graf et al., 2000;Graf et al., 2002;Roux and MacKinnon, 1999). A charged particle which moves from a highly polarizable medium such as water solution into a low polarity medium such as a protein surrounded by a lipid bilayer experiences a dielectric barrier or dielectric self-energy (DSE) (Dieckmann et al., 1999;Graf et al., 2000;Graf et al., 2002;Schuss et al., 2001). Several studies have demonstrated that transport through a narrow channel is greatly reduced or even completely inhibited by the presence of a dielectric barrier (Corry et al., 2000;Graf et al., 2000;Graf et al., 2002;Chung et al., 1999). In contrast, experimentally observed currents through narrow channels such as Gramicidin A (GA) are not negligible but, on the contrary, quite substantial - measured in tens of millions of ions per second (Hille, 1992). Therefore, these relatively small and simple molecular structures act very efficiently as ion channels. One thus suspects that a rigid model of a narrow membrane channel is inadequate for describing its ionic permeability. What is obviously missing from this oversimplified model is the motion of the channel structure itself. The importance of this aspect of ion-channel operation has been clearly demonstrated in equilibrium simulations (Roux and Karplus, 1993). In

this paper we propose a modeling approach that takes into account the dynamic implication of this motion for the transport of ions under nonequilibrium conditions. The proposed approach can describe ion currents (a long-time scale process) while accounting for the molecular flexibility of the channel protein (fast conformational changes on a short time-scale) which forms the channel. We examine the possible mechanisms by which a functional channel overcomes the impediment of a dielectric barrier and devise a model of an ion channel that is free of fitting parameters and realistic enough to yield ion currents which are compatible with experimental observations. We employ a combination of modeling methods that span a range of molecular resolutions (particle dynamics, continuum electrostatics), thus enabling treatment of ion channel permeation from first principles.

Ion permeation is slow on a molecular time scale. As an ion passes through the channel, the protein channel molecule has time to adjust its local geometry to the presence of the ion "instantaneously" on the time scale of the ion transport (Mackay et al., 1984;Partenskii and Jordan, 1992;Roux and Karplus, 1993;Tang et al., 2000;Berneche and Roux, 2000). We have performed an equilibrium MD study of protein channel relaxation with an ion placed at various positions inside the channel. Our simulations reveal that the introduction of an ion into the channel causes only small changes in the 3D structure of the protein (Woolf and Roux, 1997). These small structural changes, however, substantially alter the ion-protein electrostatic interaction energy, leading to the relative stabilization of the ion-channel complex. This observation forms the basis for the numerical approach proposed herein.

The remainder of this paper is organized as follows. In Section 2 the theoretical formulation is discussed and the simulation methods used are outlined. Section 3 describes the system studied and provides details of the numerical modeling. Our results are presented and discussed in Section 4. Section 5 concludes.

2 Theory and simulation methods

2.1 Potential of Mean Force Poisson-Nernst-Plank (PMFPNP) approach to calculate ion currents through the channel.

In continuum theory electrolyte ions are treated as a continuous electrically charged substance characterized by the concentrations $\{c_i(\vec{r})\}$ of the ionic species involved. The electric

charge of the i^{th} ionic species is denoted q_i. The distribution of these concentrations is governed by a set of drift-diffusion equations, also called Nernst-Planck equations, one for each ionic species i present in solution. In particular, $\vec{j}_i$, the flux of species i at a given point in space is given by

$$\vec{j}_i(\vec{r}) = -D_i(\vec{r})\left[\frac{\partial c_i(\vec{r})}{\partial \vec{r}} + c_i(\vec{r})\frac{\partial}{\partial \vec{r}}(\beta\psi_i(\vec{r}))\right], \qquad 1a$$

and the concentration of species i evolves in accordance with the continuity equation $\frac{dc_i}{dt} = -div\ \vec{j}_i$. In Eq. 1a D_i is the position dependent diffusion coefficient of species i, $\beta = (kT)^{-1}$ is the inverse temperature, k is the Boltzmann constant and T is the absolute temperature. Finally, $\psi_i(\vec{r})$ is the free energy of ions of species i in solution. At steady-state,

$$div\ \vec{j}_i = 0, \qquad 1b$$

and thus all quantities in Eq. 1 are time-independent. The second term on the right-hand side of Eq. 1a is the drift term due to the forces acting on a charged particle of species i from both ion-ion interactions and external sources. The latter include interactions with fixed charges on the protein system and the externally imposed electric field. Eq. 1 is supplemented by concentration boundary conditions that account for the external bulk ionic concentrations of species i (which may be different on different boundary "faces", particularly if the bathing solution concentrations on the two sides of the membrane differ).

In a continuum model $\psi_i(\vec{r})$ depends on the electrostatic charge distribution in the system and on the (generally position dependent) dielectric response function $\varepsilon(\vec{r})$. It is convenient to separate the ion free energy into two contributions:

$$\psi_i(\vec{r}) = q_i\phi_{mobile}(\vec{r}) + \Delta G^i_{SIP}(\vec{r}), \qquad 2$$

where $\phi_{mobile}(\vec{r})$ is the electrostatic potential due to all mobile ions and the applied electric field associated with external electrodes, and $\Delta G^i_{SIP}(\vec{r})$ is the potential of mean force (PMF) (McQuarrie, 1976) for a single test ion [hence "Single Ion Potential" (SIP)]. In an inhomogeneous dielectric medium $\phi_{mobile}(\vec{r})$ is determined by the Poisson equation:

$$\vec{\nabla}\cdot(\varepsilon(\vec{r})\vec{\nabla}\phi_{mobile}(\vec{r})) = -4\pi\sum_i q_i c_i(\vec{r}), \qquad 3$$

subject to Dirichlet boundary conditions, i.e., given values of the electrostatic potential are set on the boundaries of the computational box (Kurnikova et al., 1999). In reality these boundary conditions are imposed by the electrodes. In numerical models practical considerations often dictate the use of smaller subsystems, for which the computational boundary conditions need to be taken to reflect the effect of the actual ones using theoretical considerations (Graf et al., 2000). In the simplest approximation that was introduced in the field of channel modeling by Eisenberg and coworkers (Barcilon et al., 1992) the term $\Delta G^i_{SIP}(\vec{r})$ is disregarded. In an obvious generalization $\Delta G^i_{SIP}(\vec{r})$ may include the electrostatic potential due to partial charges fixed on the protein and lipid atoms, i.e. $\Delta G^i_{SIP}(\vec{r}) = q_i \phi_{protein}(\vec{r})$ (Chen and Eisenberg, 1993a;Chen and Eisenberg, 1993b;Kurnikova et al., 1999;Cardenas et al., 2000). Equations (1) and (3) are coupled nonlinearly via the c_i and ϕ_{mobile} variables. In the general case of a protein of arbitrary geometry and distribution of partial charges on protein atoms, they have no analytical solution and must be solved numerically to self-consistency (Kurnikova et al., 1999). Equations 1-3 with $\Delta G^i_{SIP}(\vec{r}) = q_i \phi_{protein}(\vec{r})$ comprise the so-called Poisson-Nernst-Planck (PNP) theory.

It was recognized recently (Roux et al., 2000;Schuss et al., 2001) that the change in solvation energy of a single ion when it moves in an inhomogeneous dielectric medium provides an important contribution to the drift flux term of Eq. 1 (Graf et al., 2002) but is missing from the PNP definition of $\Delta G^i_{SIP}(\vec{r})$ (Schuss et al., 2001;Graf et al., 2002). This change in the free energy of a single ion defined with respect to the free energy of that ion in a bulk solvent was termed the dielectric-self energy (or dielectric barrier) $\Delta G^i_{DSE}(\vec{r})$ (Graf et al., 2000;Graf et al., 2002). When the DSE is taken into account, $\Delta G^i_{SIP}(\vec{r})$ is modified to

$$\Delta G^i_{SIP}(\vec{r}) = q_i \phi_{protein}(\vec{r}) + \Delta G^i_{DSE}(\vec{r}) . \qquad 4$$

Recent studies have shown that ΔG^i_{DSE} in a narrow channel strongly influences the resulting current (Graf et al., 2000;Graf et al., 2002). Therefore, a careful assessment of $\Delta G^i_{SIP}(\vec{r})$ is essential for modeling realistic channel behavior. PNP-like theory that implements $\Delta G^i_{SIP}(\vec{r})$ as defined in Eq. 4 will be termed Dielectric-Self-Energy-Poisson-Nernst-Planck (DSEPNP) theory (Graf et al., 2002). Note that Eq. 4 still disregards a potentially important contribution to the free

energy of inserting an ion at some location in the channel that results from the corresponding change in the channel geometry.

In general, calculating free energy differences in bio-molecular processes is a challenging task. Several approaches have been adopted for various problems in molecular modeling. These theoretical methodologies span a wide range of molecular resolution—from estimating electrostatic free energies on a continuum level by solving the Poisson equation (Sharp.K.A. and Honig B.H., 1990;Dieckmann et al., 1999;Luty et al., 2002) to full atomistic Molecular Dynamics simulations (Roux and Karplus, 1993;Kollman et al., 2000). In this paper we are primarily concerned with developing a methodology to calculate $\Delta G^i_{SIP}(\vec{r})$ for an ion entering the channel which is both cost–effective in terms of computational power and can account for the most essential properties of the system (including efficient ion permeation!). Thus estimated $\Delta G^i_{SIP}(\vec{r})$ is then utilized in a PNP like kinetic theory. The general approach of combining the precalculated PMF for single ion with the self-consistent PNP approach to estimate ion currents will be termed PMFPNP.

A continuum electrostatic approach to calculate $\Delta G^i_{SIP}(\vec{r})$ is outlined in the next subsection (2.2), and a combined MD/continuum approach is presented in Section 2.3. In subsequent sections we present results of applying both methodologies to simulating current through the Gramicidin A channel, and discuss the essential physical properties that should be included in the corresponding numerical model for a realistic description of this process.

2.2 A Continuum approach to calculate the electrostatic free energy

The electrostatic free energy of transferring an ion from the bulk solution into the channel is calculated as follows:

$$\Delta G_{SIP}(\vec{r}) = G^{complex}(\vec{r}) - G^{protein} - G^{ion}, \qquad 5$$

where $G^{complex}$ is the energy of an ion plus protein/membrane complex with the ion located at a point $\vec{r}$ inside the channel, $G^{protein}$ is the energy of the protein/membrane in the absence of the ion and G^{ion} is the energy of the ion in bulk solvent.

The electrostatic energy G of a collection of point charges can be found as the $G = \frac{1}{2}\sum_i q_i \phi_i$, where the summation is over all electrostatic charges q_i in the system and ϕ_i is the value of the

electrostatic potential at the position of charge i. The electrostatic potential $\phi(\vec{r})$ needed to calculate G can be found from the corresponding Poisson equation:

$$\vec{\nabla} \cdot (\varepsilon(\vec{r})\vec{\nabla}\phi(\vec{r})) = -4\pi \sum_j q_j \delta(\vec{r} - \vec{r}_j) \qquad 6$$

supplemented by Dirichlet boundary conditions with the boundary potential set to zero. In Eq.6 δ is the three-dimensional Dirac delta-function and $\vec{r}_j$ is the position of charge q_j. We have recently shown (Graf et al., 2000;Graf et al., 2002) that for channels as narrow as 4Å in radius, a continuum description of ion permeation described by DSEPNP, i.e. Eqs. 1-6, compares well with results of Dynamic Monte-Carlo (DMC) simulations in which ions are treated as charged particles that diffuse in an inhomogeneous dielectric medium with a prescribed diffusion coefficient (Graf et al., 2002). Such particle based simulation models of narrow channels (Allen et al., 1999;Graf et al., 2000) exhibit very small superlinear currents for voltages up to 200mV. The insignificance of these currents can be traced to the presence of a DSE barrier of several kT in such channels. In contrast, real biological channels of similar size and shape exhibit substantial ionic current at low voltages, with nearly linear or sublinear current-voltage characteristics. A detailed analysis of DSEPNP and DMC particle simulations suggests that the effective polarizability of the channel environment (loosely defined as the ability of the local environment to adjust in order to stabilize an extra electric charge) must be higher than implied by the “standard” model utilized in both DMC and DSEPNP studies reported previously. Both approaches for simulating ion motions across channels suffer from two major limitations, related to the insufficient flexibility assigned to the description of the channel. First, the solvent polarizability is accounted for by a single parameter (a dielectric constant), while in reality solvent response in the confined channel environment may vary with the position in the channel in a way that cannot be determined from the bulk solvent properties. Second, the protein structure is taken to be rigid (usually at its average NMR configuration), while in reality the protein structure responds to the ionic presence. Below we will investigate the influence of both limitations.

2.3 A Combined Molecular Dynamics/Continuum Electrostatics approach to calculate free energy.

$\Delta G^i_{SIP}(\vec{r})$ can in principle be found from an atomistic simulation in which all atoms on the protein, the lipid membrane and the solvent are treated explicitly. Several attempts to calculate the

free energy of an ion in a Gramicidin A channel by MD simulation have been reported (Roux and Karplus, 1993;Elber et al., 1995), but such calculations are very difficult because they require complete sampling of the system configuration space. Since a large portion of the configuration space required for quantitative calculation of the free energy of an ion in a solvent is due to the solvent itself, it was recently proposed (Kollman et al., 2000) that the computationally expensive sampling of solvent configurations may be replaced by considering solvent effects on the mean-field level. In this approach the full-scale equilibrium Molecular Dynamics (MD) trajectory of a protein in an atomistic solvent is generated to sample the protein conformational space. The resulting sequence of protein/water configurations is used to obtain a corresponding sequence of dielectric continuum models of these systems, in which the fixed protein charges are embedded in their corresponding atomic positions. These continuum dielectric configurations, obtained with the ion fixed in a given position, are then used to compute the electrostatic free energy of inserting the ion at that position (Sharp.K.A. and Honig B.H., 1990). Following Kollman et al, 2000, the free energy of ion-protein complex formation is calculated as:

$$\Delta G_{SIP} = \frac{1}{N}\sum_{n=1}^{N}(G^{complex} - G^{protein} - G^{ion})_n \,, \qquad 7$$

where $G^{complex}$, $G^{protein}$ and G^{ion} have the same meaning as in Eq. 5 and are calculated for each protein-ion complex configuration as described in section 2.2. The index n indicates a single configuration from the MD trajectory, with N being the total number of configurations considered. This approach allows us to account for solvent effects on average, i.e. mean field level, and to reduce the noise in the free energy calculations due to insufficient sampling of solvent configurations. The procedure described above, in which the potential of mean force ΔG_{SIP} is calculated via Eq. 7 and then inputted into the PNP formalism, will be termed Potential of-Mean-Force-Poisson-Nernst-Planck (PMFPNP).

3 The simulation procedure

3.1 The model system.

The ideas outlined above were implemented in a series of calculations performed for a model Gramicidin A (GA) channel. GA is an antibiotic peptide widely used in single-channel experiments on passive ion-current permeation through a lipid membrane. It is a robust narrow channel with a relatively rigid structure. It reconstructs into a lipid bilayer by forming head-to-head

dimers of alpha-helical polypeptides. Due to its unusual primary sequence of alternating L and D amino acids it forms an alpha helix with all the amino acid side-groups extending away from the backbone helix, which forms the channel. Therefore, the channel is lined with backbone carbonyl and amino groups, generating a hydrophilic environment inside the channel. Figure 1 shows a 3D GA ion channel structure incorporated into a crude model of a lipid bilayer membrane, with the membrane/protein channel system solvated in water. This snapshot is taken from an MD simulation performed as described in the next section. As has been noted by several workers (Dieckmann et al., 1999;Roux and MacKinnon, 1999;Graf et al., 2000) the dielectric self-energy is very large for channels less than 5 Å in radius, implying the conundrum discussed above in modeling their permeability. We have chosen to work with GA, the narrowest known ion channel, to emphasize our goal of understanding the permeability of such narrow channels. It has also been pointed out (Doyle et al., 1998;Tieleman et al., 2001) that the selectivity filter of the potassium channel possesses certain similarities to the GA channel and thus our study of GA may help to understand the energetics of the potassium channel selectivity filter as well as other narrow channels.

3.2 MD/continuum simulation of an ion in the GA channel

We have performed a set of Molecular Dynamics (MD) simulations of a single potassium ion and a single chloride ion located at various positions in a Gramicidin A channel. GA was incorporated into a slab of heavy (mass=100au) spheres with Lennard-Jones parameters ε=0.05 kcal/mol and R_M=2.5 Å, and no partial charge. The slab of these dummy spheres represents a lipid bilayer by providing a non-polar environment for the channel molecule. This channel-membrane model system was then immersed in a box of 738 SPC/E water molecules. Eight water molecules in random configurations were placed inside the GA pore. This system was subjected to energy minimization followed by a 200 ps constant pressure MD equilibration run at 300 K. Positions of the dummy atoms and GA atoms were constrained in space with 200 kcal/mol/Å^2 harmonic spring forces. After the GA-water equilibration was completed, an ion (K^+ or Cl^-) was introduced into the channel. A force constant of 200 kcal/mol/Å^2 was again applied to the positions of the dummy atoms and a 10 kcal/mol/Å^2 force constant was applied to the backbone atoms of the GA. The energy of each system thus prepared was minimized, followed by a 30 ps equilibration period when the harmonic constraints on the GA backbone atoms were gradually

reduced from 10 kcal/mol/Å^2 to 0.5 kcal/mol/Å^2. Subsequently, 300 ps production runs were performed with constant volume dynamics at 300 kT. 0.5 kcal/mol/Å^2 harmonic constraints were maintained on each of the backbone C and N atoms of GA. The coordinate of the ion along the channel axis (z-axis) was held fixed, while its x,y coordinates were allowed to fluctuate. The coordinates of the protein atoms were collected every 2 ps. For every such time point along the MD trajectory the coordinates of the protein molecule and the ion were used to calculate the appropriate electrostatic free energy by solving the Poisson equation as described in Section 2.2. An MD trajectory of GA without K^+ was also generated as described above. All MD simulations were performed using the AMBER 6 software package and amber96 force field (Cornell et al., 1996). The potential parameters for the potassium ion were taken from work of Aqvist (Aquist, 1990). Bonds involving hydrogen atoms were constrained via the SHAKE algorithm. A 12 Å cut-off distance was used for all non-bonded interactions. The MD time step was set to 2 fs.

For the continuum electrostatics calculations, partial charges on the GA atoms were taken from the amber96 force field (Cornell et al., 1996). The dielectric function profile $\varepsilon(\vec{r})$ and the positions of the partial charges represent the molecular system in a continuum representation. In the numerical solution of Eq. 6, these functions are discretized on a uniform 3D grid as described in (Kurnikova et al., 1999). The radii of potassium and chlorine ions, estimated by fitting experimental enthalpies of hydration, were chosen to be R_{K^+}=2.17 Å (Dieckmann et al., 1999) and R_{Cl^-}=1.81 Å (Dasent, 1982) The electrostatic energy was calculated using our 3D PNP program (Kurnikova et al., 1999), modified to allow the assignment of several arbitrary values of dielectric constant parameters to different regions of space. For all results reported in the following sections, the grid dimensions of the simulation box were 151^3 with a linear scale of 3 grid points per Å. The width of the membrane was set to 33Å to mimic a glycerilmonoolein (GMO) bilayer. In Figure 2, a two-dimensional slice of $\varepsilon(\vec{r})$ shows how different dielectric constants are assigned to membrane (ε_m), protein (ε_p), bulk (ε_w), and channel (ε_w^{ch}) regions. The set of calculations described above was repeated with the potassium ion fixed at 18 different positions along one GA monomer at spatial increments of 1Å, and the chloride ion fixed at 7 different positions at spatial increments of 3Å. All calculations were performed on a set of IBM RS6000 workstations. It took ~12.5 hours to complete a 300 ps MD simulation and ~27 hours to solve a set of Poisson equations as prescribed by Eq. 7 for N=150.

3.3 MD calculation of the diffusion coefficients

The diffusion coefficients of the ion were calculated from the force-force autocorrelation function (McQuarrie, 1976). According to the fluctuation-dissipation theorem for a Brownian particle moving in thermal equilibrium, the 1D friction coefficient is:

$$\gamma_z(\vec{r}\,) = \frac{\beta}{2}\int_{-\infty}^{\infty} < F_z(\vec{r}\,,0)\cdot F_z(\vec{r},t) > dt \quad , \qquad 8$$

where $F_z(\vec{r},t)$ is the random force on the particle at position $\vec{r}$ along the channel axis. The space-dependent diffusion coefficient $D(\vec{r})$ for the ion can then be extracted using the Stokes-Einstein relation $D(\vec{r}) = \left(\beta\gamma(\vec{r})\right)^{-1}$.

The input needed for Eq. 8 was obtained from equilibrium MD simulations with the potassium ion fixed in space. Starting with equilibrated systems of K^+ fixed in the GA channel at a particular position along the channel axis, a 1 ns trajectory was generated and the forces acting on the ion were collected. This calculation was repeated at 18 K^+ ion positions selected as indicated above. A similar MD simulation of a potassium ion in bulk water was also performed. In the latter simulation the K^+ ion was immersed in a box of 735 SPC/E water molecules, the system was equilibrated, and finally, a 1 ns constant volume equilibrium trajectory was generated.

4 Results and discussion

4.1 Continuum dielectric theory: the role of the dielectric response

In continuum modeling of biological channels the position dependent dielectric response function plays a prominent role. The most common choice for the dielectric constant of the membrane and the protein molecule is $\varepsilon_m=\varepsilon_p$=2-5. Water is usually represented as a dielectric medium with dielectric constant ε_w=80. The choice of these parameters for calculating electrostatic free energies of binding in solution has been intensively scrutinized in recent literature on globular proteins and organic molecules (Nosjean et al., 1997;Simonson and Brooks, 1996;Sharp.K.A. and Honig B.H., 1990;Warshel and Russell, 1984). However, the appropriate choice of dielectric constants for membrane proteins and membrane environments is relatively unexplored. We have examined the dependence of the electrostatic binding free energy $\Delta G_{SIP}^{K^+}$ in the GA channel, calculated as described in Sec. 2.2, on the choice of the dielectric constant values of the channel

environment (as in Fig. 2). Indeed, the two-ε model predicts a huge solvation barrier for an ion in a narrow channel. Figure 3 shows via the solid line with filled circles $\Delta G_{SIP}^{K^+}$ for a potassium ion in a GA channel, as a function of the ion position along the channel axis, for a set of ε values in the range indicated above, namely, $\varepsilon_w=\varepsilon_w^{ch}=80$, $\varepsilon_m=\varepsilon_p=4$. The 3D channel structure reported by (Arsen'ev et al., 1986) was employed in these calculations. Note the high barrier of ~14kT to bring the ion into the center of the channel which results from this choice of parameters. Such a barrier would completely block ion current (Graf et al., 2002) in contrast to experimental observation. Since the GA channel is very efficient in passing simple cations, one should ask what other properties of the channel and its environment must be incorporated into the model to describe its interaction with the ion at least qualitatively correctly. It is widely believed that the environment around a biological channel is highly inhomogeneous in its electrostatic properties and therefore cannot be described adequately by just two dielectric constant regions. One possibility is that simply employing a better description of the dielectric response function may yield a more realistic permeability model. A protein is a polarizable medium and ε_p values between 4 and 20 have recently been suggested to represent a protein molecule* (King et al., 1991;Gilson and Honig B.H., 1986;Schutz and Warshel, 2001). Therefore, the dielectric constant ε_p was increased in several increments up to $\varepsilon_p=30$, keeping $\varepsilon_w=\varepsilon_w^{ch}$ and ε_m as 80 and 4, respectively. Fig. 3 shows results for $\Delta G_{SIP}^{K^+}$ obtained under these conditions. We see that even for ε_p as high as 30 the barrier $\Delta G_{SIP}^{K^+}$ is still ~2.5kT. Note that the mobility of water inside the channel is highly restricted and its dielectric response is probably substantially lower than that of bulk water. Still, we find that the ion penetration free energy is rather insensitive to the water dielectric constant value in this region. This is shown in Table 1, in which ε_w^{ch} was varied between 40 and 200. It appears that for a narrow channel confined within a low dielectric constant (ε<6) membrane, a substantial dielectric

* It should be emphasized that this separation of the single ion potential into two contributions, one associated with explicit charges in the environment (in this case the protein) and the other arising from the dielectric self energy, is to some extent arbitrary and reflects our choice of the electrostatic model for the protein. When partial charges on the protein are treated explicitly the background environment is characterized by a low (2-4) dielectric constant. Alternatively the protein is sometimes treated as a high dielectric constant environment thus accounting for partial charges that are not treated explicitly. In the latter case the term will not appear in Eq. 4.

barrier exists even if the protein and/or the channel region are assigned unphysically high dielectric constants. Our recent DMC studies of ion current in a model cylindrical channel (Graf et al., 2000) indicate that an energetic barrier as low as 2 kT effectively inhibits any appreciable ionic current at low applied voltages (Graf et al., 2000;Graf et al., 2002). Therefore, other mechanisms by which the environment can polarize in response to the presence of a permeating ion must exist. As outlined in Section 1, a likely mechanism entails local conformational changes in the protein as the ion moves through the channel. The next sub-section considers this possibility.

4.2 Free energy of Ion-Channel association from combined MD simulations and continuum electrostatics method: The role of channel relaxation

In order to elucidate the influence of the protein molecule itself on the passage of an ion through the channel, the free energy $\Delta G_{SIP}^{K^+}$ associated with transferring a K^+ ion from the bulk electrolyte solution to a particular point $\vec{r}$ inside the GA channel was calculated as described in sections 2.3 and 3.1, i.e., a sample of GA configurations was obtained from equilibrium MD simulations with a K^+ ion at various positions along the channel, followed by continuum dielectric model calculations of the free energy associated with transferring the potassium ion into the channel. The results obtained from these simulations are shown in Figures 4-7. Figure 4 shows $\Delta G_{SIP}^{K^+}$ as a function of time calculated along the MD trajectory for the complex with the ion positioned in the center of the channel as in Fig. 1, starting from an initial protein structure taken as the NMR geometry. The values of the dielectric constants used in the electrostatic part of this calculation are ε_p=2, ε_m=4, ε_w^{ch}=40 and ε_w=80. The initial relaxation of energy at the onset of the simulation is shown in Figure 4a. The free energy drops below zero on average in a fraction of a pico-second. This result clearly demonstrates the short time-scale required for the protein to adjust to the insertion of the ion. The equilibrium state is reached after a longer time. Electrostatic calculations in the equilibrated part of the trajectory, presented in Figure 4b, were performed using ε_p=4 (solid line) and ε_p=2 (dashed line), keeping ε_m and ε_w^{ch} as above: note that $\Delta G_{SIP}^{K^+}$ is characterized by large fluctuations between positive and negative values. That is, the protein fluctuates between “permeable” and “non-permeable” structures in rapid succession. On average, however, more configurations that favor ion binding inside the channel occur and the resulting average energy is negative, i.e. favorable for ion permeation into the channel. Another important

observation that can be drawn from Fig. 4b is that the dependence of the calculated energy on the value of ε_p is different for different configurations. For some structures e.g. the initial NMR structure, $\Delta G_{SIP}^{K^+}$ increases as ε_p decreases in the same manner as observed in Fig. 3. For others, however, the energy decreases with decreasing ε_p, resulting in tighter binding of a complex. This is somewhat counterintuitive and demonstrates that for any particular spatial distribution of the dielectric response function ε® it is impossible to predict a priori how the polarization of the media around the charge will influence the calculated electrostatic energy in the system. The dependence of $\Delta G_{SIP}^{K^+}$ on the choice of ε_w^{ch} and ε_m is shown in Figures 5a and 5b respectively for several snapshots from the MD simulation. $\Delta G_{SIP}^{K^+}$ depends very weakly on ε_w^{ch} (see Fig. 5a) and varies monotonically with ε_m (Fig. 5b).

$\Delta G_{SIP}^{K^+}$ was shown for individual channel configurations in Figures 3-5, in what follows we consider the corresponding free energy averages over the entire equilibrium MD trajectory according to Eq. 7. The following values of dielectric parameters were used in the remainder of the paper: $\varepsilon_m=\varepsilon_p=4$, and $\varepsilon_w=\varepsilon_w^{ch}=80$. Figure 6 shows this trajectory-averaged free energy as a function of ion position along the channel axis. Deep wells in the $\Delta G_{SIP}^{K^+}$ profile indicate cation stabilization (and thus possible ion binding sites). The energy minima located closer to the entrance to the channel are deeper than the two energy minima near the center of the channel. It is important to emphasize the large difference between the free energy for ion insertion calculated for the relaxed channel and for the NMR configuration. In Figure 7a the averaged $\Delta G_{SIP}^{K^+}(\vec{r})$ in the relaxed channel is shown (again) along with $\Delta G_{DSE}^{K^+}(\vec{r})$. The electrostatic free energy of transferring an ion from the bulk solution into the channel for the NMR channel geometry, calculated in the same manner, is shown in Figure 7b. It is clearly seen that the relaxation of the channel environment during the MD simulation leads to a huge decrease in the cost of introducing an ion into the channel. If the channel is kept in its NMR geometry, an ion entering the channel experiences an energetic barrier. Thus, it is favorable for the ion to bind into the channel if the channel is allowed to relax in response to the ion's presence. This relaxation evidently leads to a dramatic decrease of the electrostatic free energy, which may become negative. Further inspection of the DSE term in Fig. 7 (diamonds) and the total $\Delta G_{SIP}^{K^+}(\vec{r})$ (circles) reveals that when channel flexibility is allowed (Fig.

7a) only minor changes in the dielectric-self-energy (DSE) term occur, whereas the total complex association energy $\Delta G_{SIP}^{K^+}(\vec{r})$ decreases significantly. The latter observation indicates that for our choice of the electrostatic model of the protein (see Footnote *) the main effect of the small structural changes in the channel molecule is to modify the direct electrostatic interactions of the permeating ion with the partial charges on the protein groups. The effect of protein relaxation on $\Delta G_{DSE}^{K^+}(\vec{r})$ is small. The direct ion-protein electrostatic interactions become significantly stronger in a flexible channel and can compensate the large DSE, thus rendering the channel permeable. Next, we investigate how the structure of the protein is on average affected by the ion's presence in the protein channel. The central part of the GA channel is formed when two alpha-helical monomers are stacked on top of each other in the membrane. They are held together only by hydrogen bonds, and therefore the center is the most flexible part of the channel, which is fairly rigid in other parts (Woolf and Roux, 1997). We have found that deviations from the average atom positions due to the ion presence are fairly small even in the center of the channel. Therefore, we report only the results corresponding to the ion position in the center of the channel to demonstrate that the influence of the ion on the channel structure is small even in this case. In Figure 8 the root mean square deviation (RMSD) from the average equilibrium geometry of the backbone carbonyl oxygen atoms lining the channel pore, accumulated over the course of the MD simulation, is shown. By comparing the RMSD for channels simulated with and in the absence of K^+ ion one can also conclude that the average geometry of the protein molecule remains unchanged as the ion is introduced into the channel. Direct comparison of the NMR and average MD structures indeed reveals only small changes in the average positions of the protein atoms. This is further illustrated in Figure 9, where we have superimposed the average MD coordinates of the GA-K^+ system with the average MD coordinates of the GA system. It can be seen from this figure that the largest changes in atomic positions between the two structures occur for carbonyl oxygen atoms closest to the ion. In particular, carbonyl groups near the ion have tilted towards it, as indicated by arrows. Other workers studying narrow channels, e.g. GA and K^+ channels (Mackay et al., 1984;Roux and Karplus, 1993;Shobana et al., 2000;Nina et al., 2000;Tang et al., 2000) have observed that ions distorted the positions of the carbonyl oxygens to achieve proper solvation. The average positions of most other GA atoms have not changed significantly. Table 2 reports the largest average distances and magnitudes of distortion between the potassium ion and

the nearest carbonyl oxygens when the ion is in the center of the GA channel. There are four carbonyl oxygens whose distances from the ion decrease substantially when the ion is introduced into the center of the GA. Even for the largest distortions reported here, it can be seen that the hydrogen bonds among the backbone atoms of GA remain intact, i.e. the additional tilt angle of carbonyl groups involved remains small (see Fig.9).

The shape of the free energy profile in Fig. 6 suggests that there are four energy wells in the GA channel. Two of them, represented by the deeper minima, are located at a distance of ~9 Å from the center of the channel. This observation agrees well with previous experimental and theoretical studies of GA binding sites (Woolf and Roux, 1997;Kurnikova et al., 1999;Im et al., 2000). Two other, energetically shallower, energy minima reside approximately 3Å from the center of the channel (Kurnikova et al., 1999).

Finally we consider the free energy profile for a chloride ion in the GA channel. As in the K^+ case, when the GA channel is allowed to relax as described above the free energy barrier calculated for a Cl^- ion decreases (see Fig. 10). However, the magnitude of the net barrier in the center of the channel is still much too large to expect any significant Cl^- current through the channel.

4.3 Calculation of diffusion constants

Current calculations using PMFPNP or Brownian Dynamics techniques crucially depend on the magnitude of the diffusion coefficients that characterize the motion of ions in the channel. In the narrow pore of Gramicidin the permeant ion is largely desolvated and is instead coordinated by backbone carbonyl groups. The mobility of the permeating ion is suppressed not only by the restrictions inherent in its lateral confinement but also by strong electrostatic interactions with these carbonyl oxygens. Moreover, due to the single file arrangement of the ion and water molecules, the motion of the ion is coupled to the motion of surrounding water. The mobility of water is also inhibited inside the channel (Elber et al., 1995;Hinsen and Roux, 1997).

There are no direct experimental measurements of diffusion coefficients of ions inside Gramicidin or other channels. The diffusion coefficient of a potassium ion in bulk water calculated as described in section 3.3 and indicated in Figure 11 is only 13% smaller than the experimentally measured value (Lide 1994). The calculated diffusion coefficient of a K^+ ion inside the channel is ~8.5 times less than in the bulk solution (again, cf. Fig. 11). Several model MD studies of ion diffusion coefficients inside various model channels have been reported recently. All of them find

reduction by a factor of 3-10 in the diffusion coefficient when the ion is moved from bulk water into a channel environment (Lynden-Bell and Rasaiah, 1996;Nina et al., 1999;Smith and Sansom, 1999). Furthermore, the ion's mobility is expected to be position dependent. Figure 11 shows the dependence of $D_{ch}^{K^+}$ on the position of the ion in the channel (distance is measured with respect to the channel center). One can see that when an ion leaves the channel (at about 17Å from the channel center) its diffusion coefficient abruptly increases by a factor of four. At this distance the ion is completely solvated by reservoir water and spatial correlation with the channel is very weak. The small size of the simulation box did not allow us to move the ion to a distance from the channel at which the value of the bulk $D_w^{K^+}$ is completely recovered. Based on the numerical results shown in Fig. 11 we have used $D_w^{K^+}$ =1.75x10^{-5} cm^2/s in the bulk region and 0.25x10^{-5} cm^2/s in the channel with a linear interpolation function connecting bulk and channel diffusion constant at the ends of the GA.

4.4 Ion current

With the calculated diffusion coefficients and free energies for ion–channel interaction in hand we can now apply the PMFPNP procedure, as prescribed by Eqs. 1-7, to evaluate ion currents in the GA channel. The 1D potential along the (z) channel axis extracted from MD/continuum calculation was simply extended in the lateral (x,y) directions. Within the narrow channel, variation in the lateral direction is expected to be minor, and likewise in the bulk solution regions. Near the channel entrances, the SIP will not be strictly independent of x,y position, but again, we expect the error in the I-V curves resulting from the simplified SIP profile employed here to be negligible. The SIP profiles shown in Figures 6 and 10 were used for the K^+ and Cl^- ions, respectively. The dielectric constants were set to $\varepsilon_m=\varepsilon_p=4$, and $\varepsilon_w=\varepsilon_w^{ch}=80$. In Figure 12 the current-voltage characteristic of a GA channel in a GMO membrane is shown for two values of reservoir electrolyte concentrations. The inset to Figure 12 displays experimental measurements of single ion channel currents for this system (Busath et al., 1998). Our calculated currents compare rather well with the experimental curves. At 200 mV applied voltage the theory underestimates measured currents for the low bath electrolyte concentration (0.1M) by about a factor of two. Given that no fitting parameters were employed in our analysis, the agreement with experiment is respectable. We note that one possible source of error is underestimating the

diffusion constant values, and further studies regarding the validity of the procedure that uses Eq. 8 in the restricted channel environment are required.

In Figure 13 ion current is plotted as a function of the reservoir electrolyte concentration (IC characteristic) at an applied voltage of 100mV. At V=100mV the experimental current data points shown in Fig. 12 at concentrations up to 2M are consistently 2-3 times larger than the prediction of our PMFPNP calculations, thus implying a similar trend towards saturation. As noted above, we have chosen not to scale our results, although the diffusion coefficients calculated from MD might be underestimated. The saturation of IC curves is not observed in simple PNP theory, i.e. with $\Delta G_{DSE}^{K^+} = 0$ and a rigid channel (as demonstrated by the line with diamonds in Fig. 13). In order to understand the mechanism of saturation in PMFPNP we have plotted the free energy $\psi_i(\vec{r})$ along the channel axis that results from PNP (Fig. 14a, c) and PMFPNP (Fig. 14b, d) for several bulk electrolyte concentrations. By comparing Figs. 14a and 14b we observe that the potential profile features several barriers for the positive ion in PMFPNP. The height of the barriers increases as the bulk electrolyte concentration increases. In standard PNP, however, such barriers are not observed (Fig. 14a). In PMFPNP (see Figs. 14b, d) negative ions experience a much larger barrier than positive ions in the channel. As indicated in Figure 15, when the bulk ion concentration increases, the positive ion density in the channel also increases and cannot be compensated by negative ions. The resulting effective positive charge in the channel creates a larger effective barrier for the transfer of positive ions and leads to current saturation with increased salt concentration. However, since PMFPNP does not account for the direct ion-ion dynamic correlations, it may only partially account for correlation-dependent phenomena such as currents at large bath electrolyte concentrations at high voltages. Clearly, the nature of direct ion-ion correlations in a channel environment is not completely understood and requires further study.

5 Conclusions

The passage of ions through narrow membrane channels is affected by a combination of interconnected energetic and kinetic factors including the local electric field resulting from the response of the membrane and the channel protein to the externally imposed potential, the energetics (electrostatic and short range interactions) of the ion accommodation in different parts of the channel, the electrostatic interaction between mobile ions in and near the channel and the

ions mobilities in the channel environment. Full-scale MD simulations of this phenomenon are not yet practical because of the vastly different time and length-scales involved.

Alternative simplified coarse-grained models have tried to capture the essential physics of the process. The Poisson-Nernst-Planck (PNP) approach focuses on the electrostatic interaction between permeant ions and between one such ion and its rigid inhomogeneous dielectric environment as the main factors that control the channel operation. Calculations of ion transport through the Gramicidin A (GA) channel based on this approach have shown a remarkable agreement with experimental results(Kurnikova et al., 1999;Cardenas et al., 2000;Hollerbach et al., 2000). The present calculations together with several recent works show, however, that this apparent success is an artifact resulting from the cancellation of two errors that are big for narrow channels such as GA. First, the PNP approach strongly underestimates the dielectric barrier associated with transferring an ion from bulk water into the channel. This would lead to a strong overestimate of the ion current. Second, the PNP model considers the channel protein and the membrane as rigid dielectric environments, disregarding the channel structural response to the presence of the ion and thus implying a relatively small ability of the channel to accommodate the ion and to facilitate its transfer. This alone would lead to the opposite effect of underestimating the ion current. These two errors compensate each other in the final result for ion transport through the GA channel.

In the present paper we have described a hybrid molecular dynamics-continuum electrostatic methodology that makes it possible to combine the convenience and numerical efficiency of a PNP-based calculation with correct accounting for dielectric barrier and channel relaxation effects. This methodology contains several ingredients:

(1) The water, membrane, protein and channel environments are modeled as dielectric continua. Uncertainties regarding the dielectric constant of the protein are avoided by explicitly describing the partial charges on the protein backbone. The remaining protein then responds as a low dielectric constant (hydrocarbon-type) environment, as does the peptide membrane.

(2) The standard PNP approach is corrected by adding the gradient of a suitable single-ion potential to the drift term in the drift-diffusion equation 1. In another work (Graf et al., 2002), in which this potential has been derived from the dielectric response of a rigid membrane-protein complex to the presence of a single ion, we have shown that this approach provides a good approximation for the dielectric barrier.

(3) This electrostatic single-ion potential is further augmented by a contribution arising from the channel structural response to the ion. This is done by using atomistic MD simulations to compute this response, while still maintaining numerical simplicity by representing the resulting responsive structure as a dielectric continuum for the purpose of computing the local electrostatic energy.

(4) The local diffusion coefficient of the ion is obtained from a first-principle calculation based on MD evaluation of the force-force autocorrelation function associated with the ion positioned at different locations along the channel.

(5) The modified PNP equations, including all the above ingredients, now referred to as the Potential of-Mean-Force-Poisson-Nernst-Planck (PMFPNP) model, are used to calculate the ionic current for the imposed potential and concentration biases.

We have seen that this calculation yields results that agree well with available experiments on ion transport through the GA channel, without employing any arbitrary adjustable parameters. This suggests that the present modeling indeed accounts for all essential factors that potentially affect ion transport through open membrane channels. Still, one must view this success with some caution. The use of continuum dielectric models for the protein and water with the inevitable introduction of ill-defined dielectric constants and the neglect of restrictions on water mobility in the channel is obviously a serious approximation. Also, dynamic correlations between ions in the channel that possibly affect the dynamics of ion permeation, especially at higher concentrations, are only partially accounted for by this model. Further experimental and computational work is needed to fully assess the model reliability.

Acknowledgements

AN's work was supported in part by the Israel Science Foundation and by the Kurt Lion Fund. Work in RDC's group was supported by NIH Grant R0l GMG1082-03 and ACS-PRF grant 34754-AC6. The calculations reported here were carried out on computers at the University of Pittsburgh's Center for Molecular and Materials Simulations (CMMS).

Figures

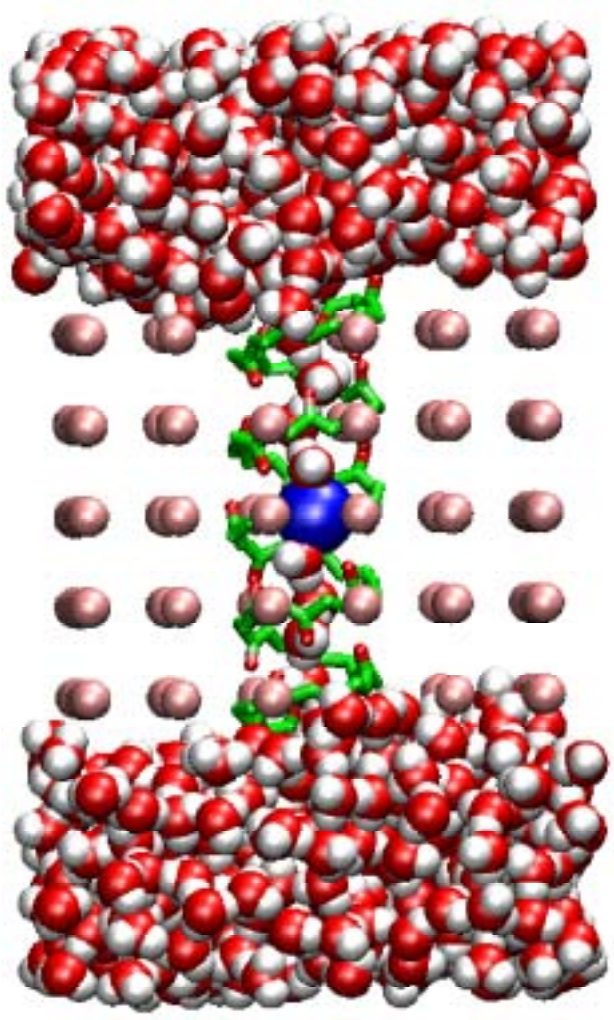

Figure 1. Snapshot of the GA channel with a K^+ ion embedded in a model membrane and solvated with water after a 300 ps MD simulation as described in text. The model lipid bilayer is represented by violet spheres (the radius of the violet sphere in a picture does not reflect its Lennard-Jones parameters). The K^+ ion is shown as the blue sphere in the center of the channel. Only backbone atoms of the peptide chains are shown.

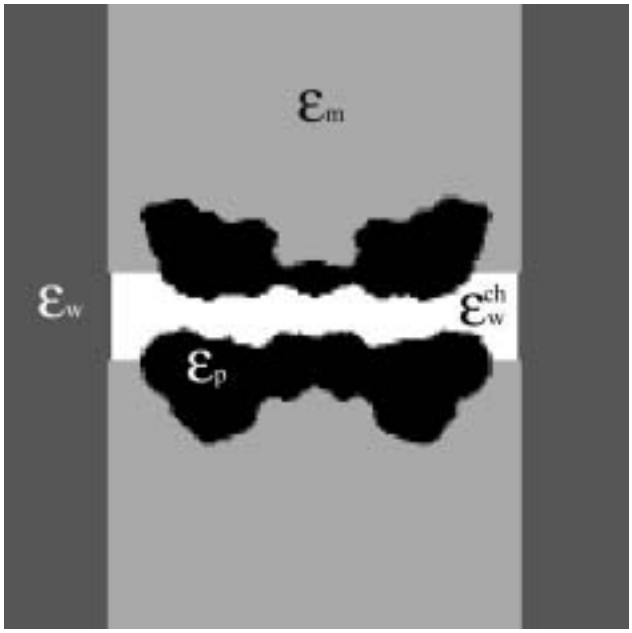

Figure 2. 2D center-cut of the 3D space-dependent dielectric constant function used for numerical solution of the Poisson equation. The simulation system is divided into four regions: the protein and the ion (ε_p), the bulk water (ε_w), the membrane (ε_m) and the channel water (ε_w^{ch}).

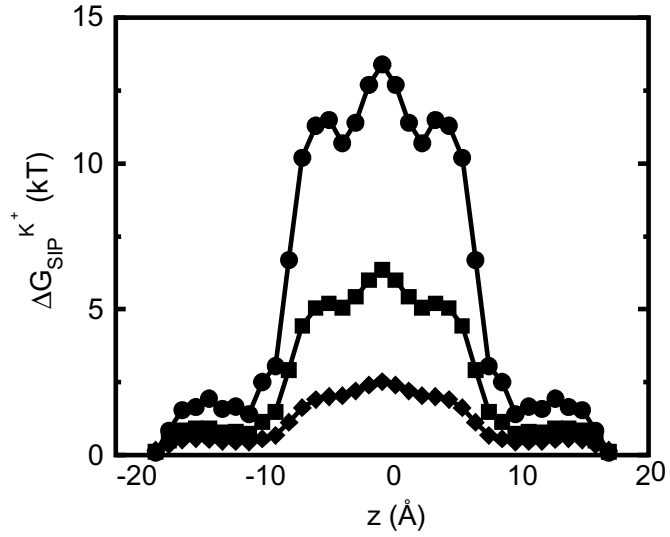

Figure 3. Electrostatic free energy of the K^+-GA binding $\Delta G_{SIP}^{K^+}$ plotted as a function of the ion displacement from the center of the GA channel along the channel axis. The energy is calculated by numerical solution of the Poisson equation for a configuration of GA taken from the PDB data bank (Arsen'ev et al., 1986) (Eq. 5-6). The dielectric constant of the bulk water is ε_w=80, the membrane ε_m=4 and the channel water ε_w^{ch}= 80. The dielectric constant of the protein was taken to be ε_p=4 (●), 10 (■) and 30 (♦). See Fig. 2 for the assignment of regions with different dielectric constants.

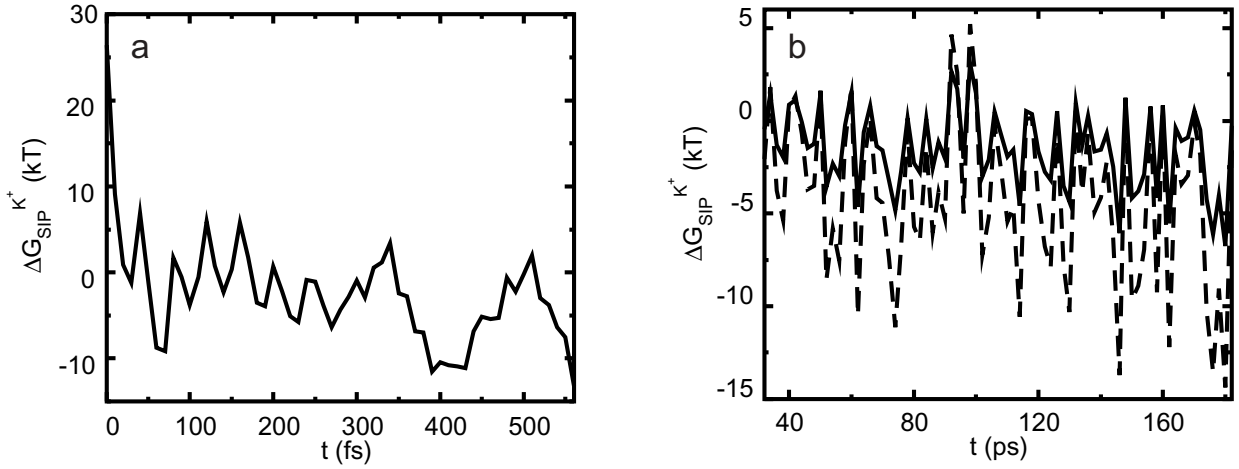

Figure 4. $\Delta G_{SIP}^{K^+}$ calculated for different protein structures which are collected during the MD simulation. Note how the energy fluctuates between positive and negative values, indicating ion-permeable and impermeable structural conformations of the protein (see explanation in text). In both panels ε_w^{ch}=40, ε_w=80, ε_m=4 a) Initial relaxation. ε_p=2. b) A portion of the equilibrium trajectory. Solid line shows the calculations with ε_p=4 and dashed line is for ε_p=2.

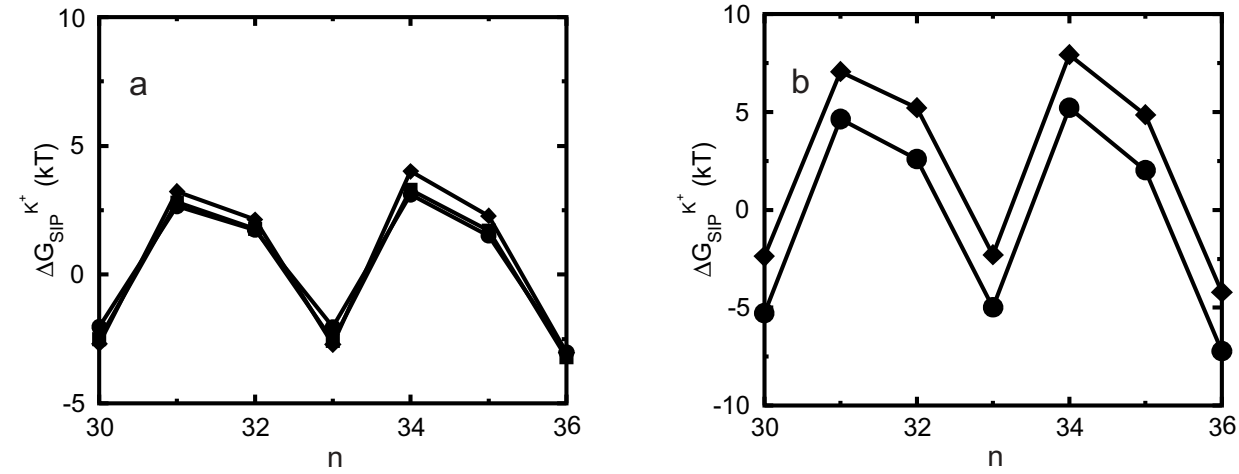

Figure 5. a) Dependence of $\Delta G_{SIP}^{K^+}$ on ε_w^{ch} plotted for several snapshots taken from the MD trajectory. n is the index labeling snapshots along the MD trajectory. The following set of dielectric parameters was used ε_p=ε_m=4, ε_w=80. The dielectric constant of the channel water was set to ε_w^{ch}=20 (♦), 40 (■) and 80 (●). See Fig. 2 for the assignment of regions with different dielectric constants. b) Dependence of $\Delta G_{SIP}^{K^+}$ on ε_m plotted for several snapshots taken from the MD trajectory. The following set of dielectric parameters was used ε_p=2, ε_w=80, ε_w^{ch}=40. The dielectric constant of the membrane was set to ε_m=2 (♦) and 4 (●).

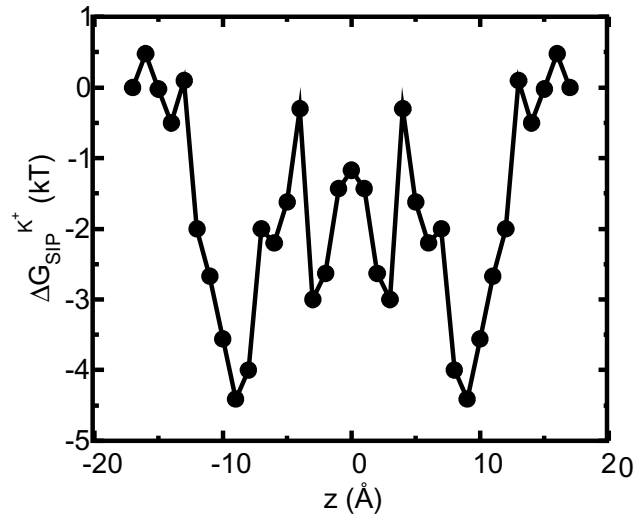

Figure 6. Average $\Delta G_{SIP}^{K^+}$ for a flexible protein. Each point in the plot is the average of N=150 calculations along the 300 ps MD trajectory as prescribed by Eq 7. The following set of dielectric parameters was used: $\varepsilon_p=\varepsilon_m=4$, $\varepsilon_w=\varepsilon_w^{ch}=80$.

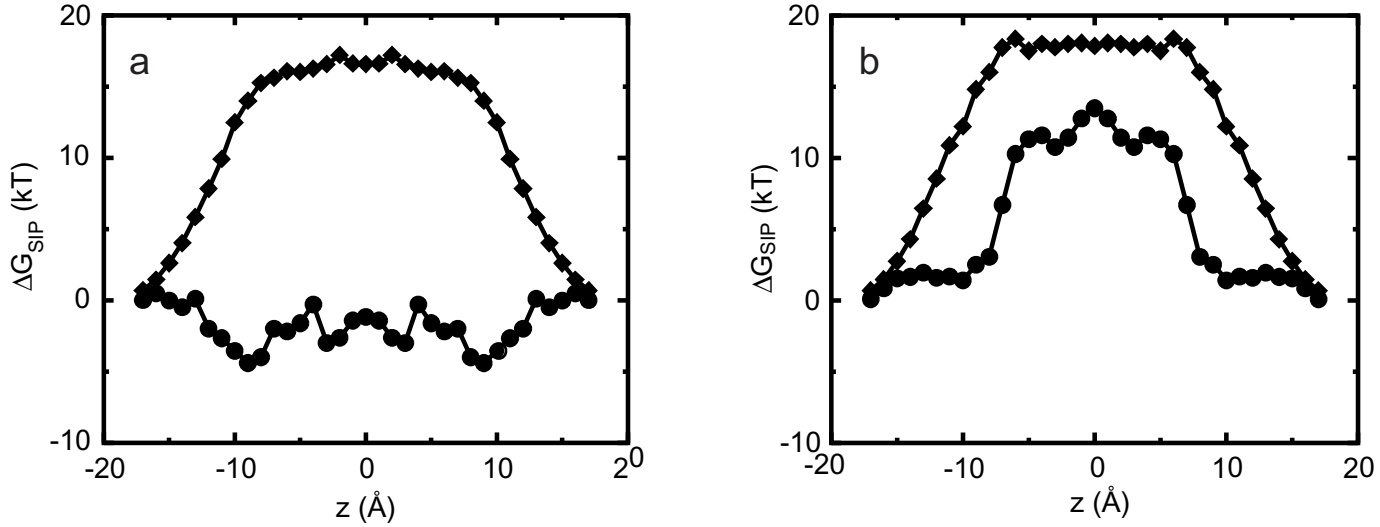

Figure 7. **a**) Average free energy of K^+-flexible GA binding $\Delta G_{SIP}^{K^+}$, i.e. with partial charges on GA atoms (●), and $\Delta G_{DSE}^{K^+}$, i.e. without partial charges on the GA atoms (♦). Each point is the average of N=150 calculations along the 300 ps MD trajectory as prescribed by Eq. 7. **b**)The same as in (a) but for the rigid NMR geometry of GA as prescribed by Eq. 5.

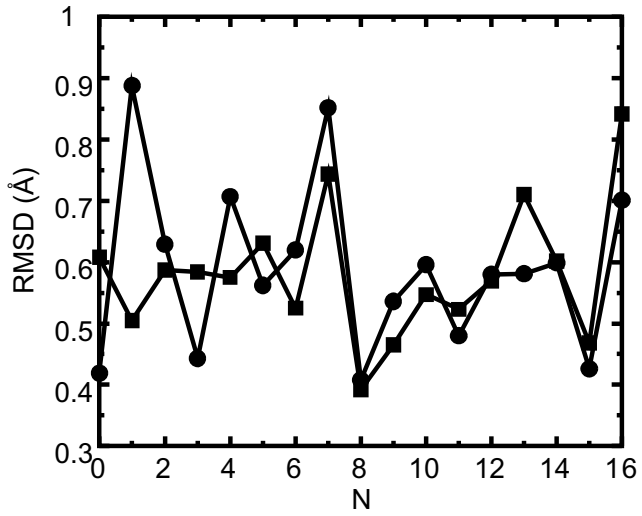

Figure 8. Root Mean Square Deviation (RMSD) of GA backbone carbonyl oxygen atoms in the MD simulation. The numbers of the residues in the protein sequence are indicated on the abscissa. Circles correspond to the simulation with a K^+ ion placed in the center of the channel (●). The curve with the squares is for the GA channel without K^+ (■). Each RMSD curve is calculated along the 300 ps MD trajectory relative to the corresponding average MD structure.

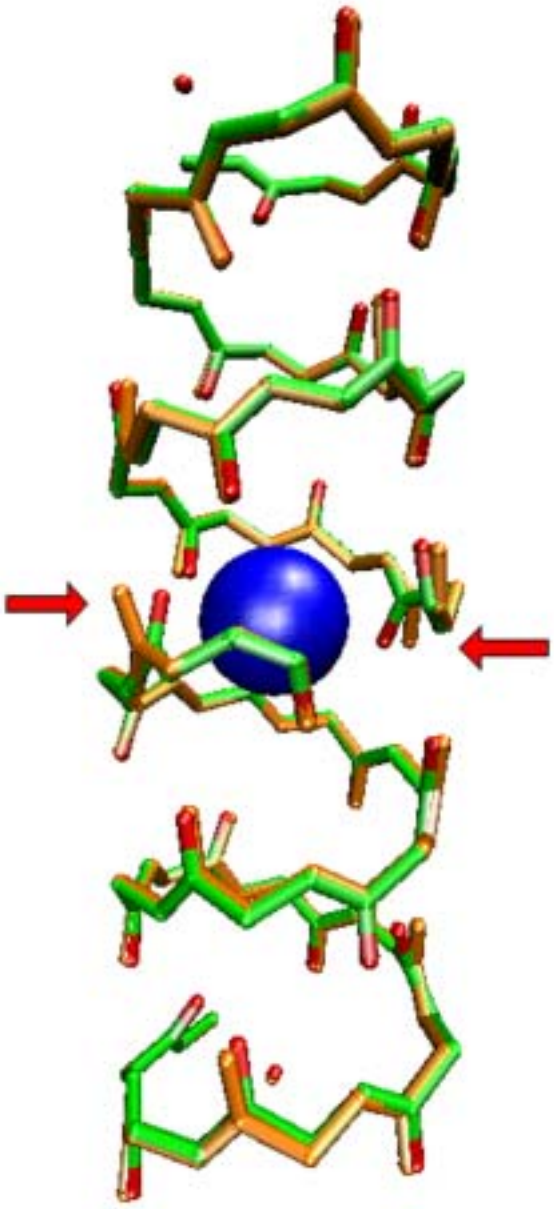

Figure 9. Two GA protein structures are superimposed. Orange peptide is the structure calculated as an average over the MD trajectory of the flexible GA channel without K^+. The second structure is for the K^+-flexible GA complex with coordinates averaged over the MD trajectory. Only the backbone atoms of the GA peptide are shown. K^+ is represented by the blue sphere in the channel center. Arrows indicate the carbonyl oxygens that bend toward the K^+ ion due to favorable electrostatic interactions.

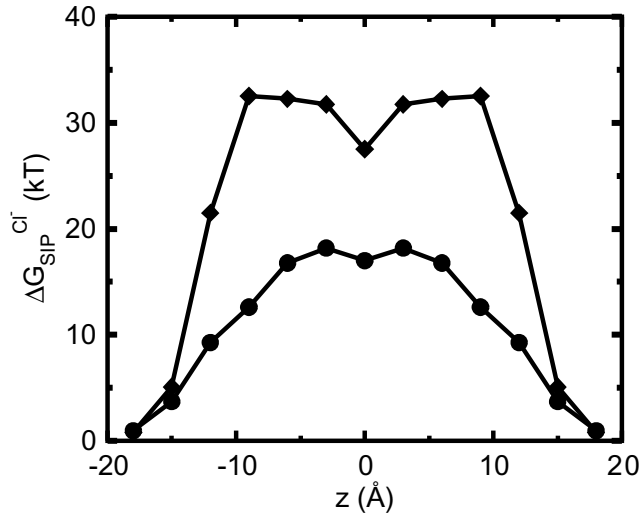

Figure 10. Average $\Delta G_{SIP}^{Cl^-}$ for a flexible GA (●) and for a rigid one (♦). For the flexible protein each point in the plot is the average of N=150 calculations along the 300 ps MD trajectory as prescribed by Eq 7. The NMR geometry of the GA was used for the rigid channel. The following set of dielectric parameters was used for both calculations: $\varepsilon_p=\varepsilon_m=4$, $\varepsilon_w=\varepsilon_w^{ch}=80$.

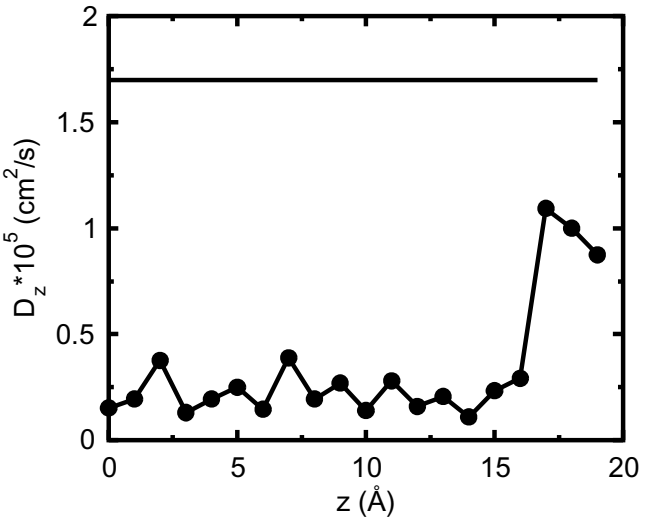

Figure 11. Calculated diffusion coefficient for K^+ ion inside of the GA channel (●), and in bulk SPC/E water (solid line). Only the D_z component of the diffusion coefficient of the ion in the channel is calculated.

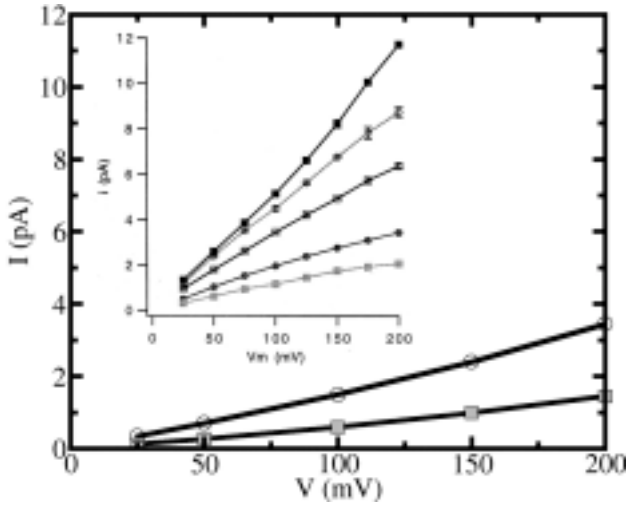

Figure 12. Current-voltage relations predicted by PMFPNP model are compared to experimental results (Busath et al., 1998) (upper left inset). Bulk KCl concentrations of 0.1 (shaded square) and 1.0 M (open circle) were used in the simulations. The experimental curves in the inset correspond to the following concentrations of bulk KCl solutions: shaded square-0.1M, filled circle-0.2M, open square-0.5M, open circle-1.0M and filled square-2.0M. The analogous experimental and calculated curves are labeled with the same symbols.

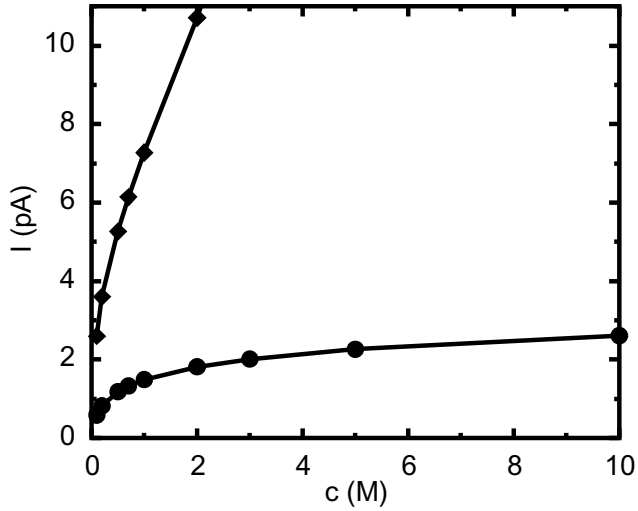

Figure 13. Current-Concentration relations as predicted by PNP (♦) and PMFPNP (●) models. The external potential difference was set to 100mV.

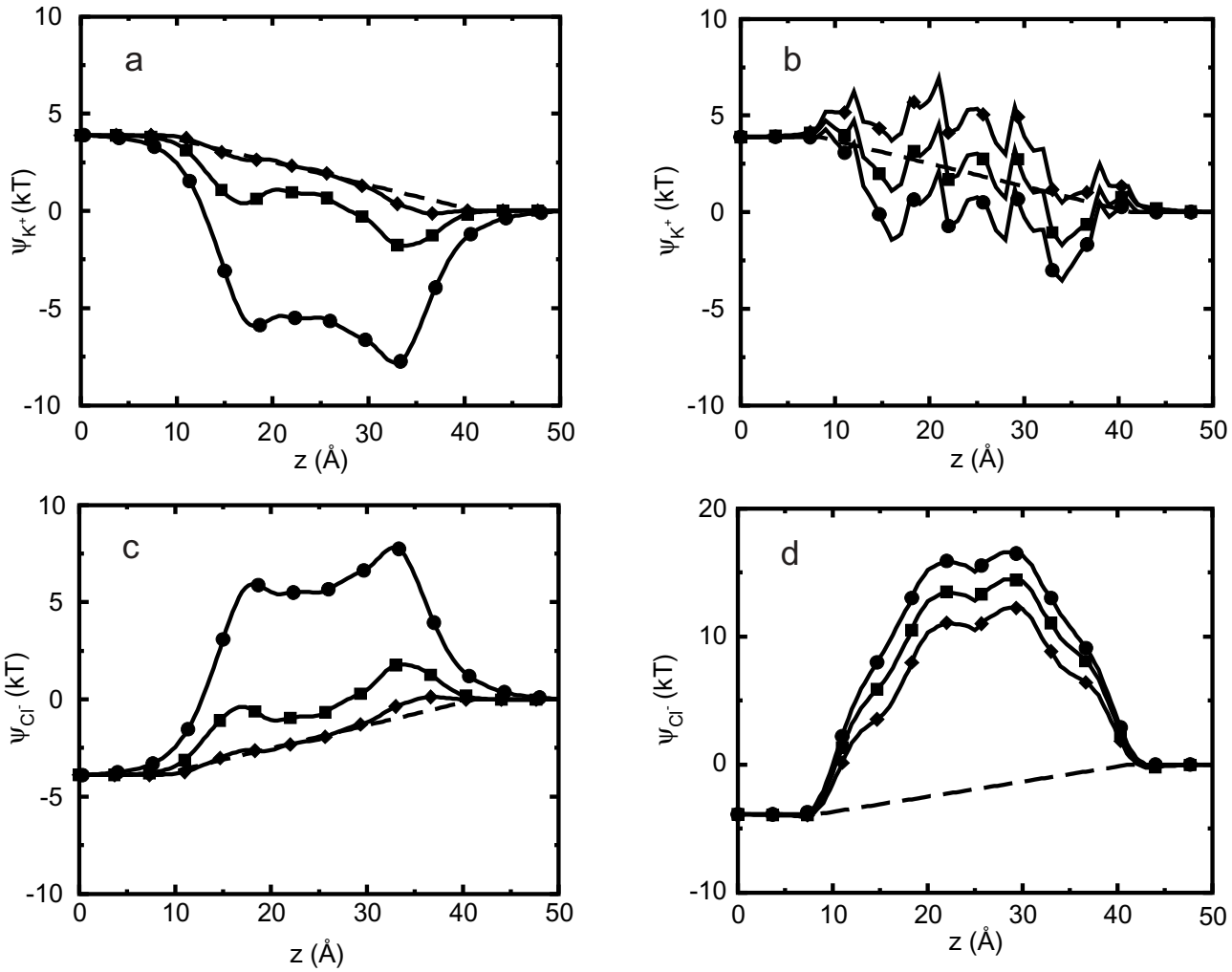

Figure 14. $\psi_i(\vec{r})$ profile along the channel axes for K^+ and Cl^- is plotted for several bulk electrolyte concentrations and 100mV applied voltage: a), c) calculated using PNP; b), d) calculated using PMFPNP. The curve with circles is for 0M, the curve with squares is for 0.5M and the curve with diamonds is for 10M electrolyte concentrations. The dashed line is the result of the calculation in which protein molecule had no partial charges on the atoms. It corresponds to the linear ramp potential caused by the high resistivity of the membrane.

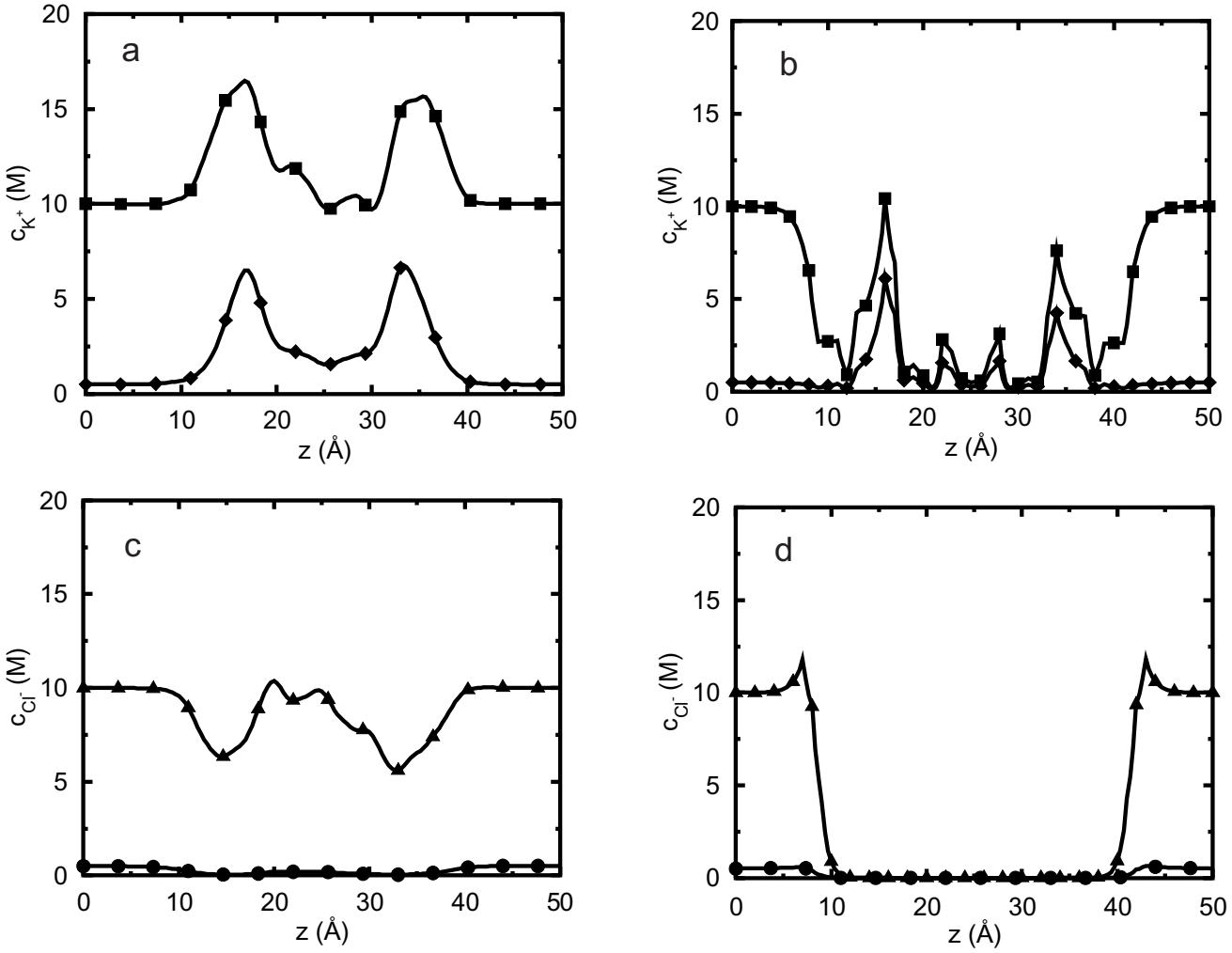

Figure 15. Ion concentration profile along the channel axis for K^+ and Cl^- is plotted for several bulk electrolyte concentrations: a), c) calculated using PNP; b), d) calculated using PMFPNP. The curves with diamonds and circles are for 0.5M, the curves with squares and triangles are for 10M electrolyte concentrations.

Tables

Table 1. The value of the $\Delta G_{SIP}^{K^+}$ barrier calculated by numerical solution of the Poisson equation for a rigid NMR configuration of GA (as prescribed by Eq. 5). The dielectric constant of the channel water is varied while dielectric constants of other parts of the system are kept fixed with epsilon of bulk water ε_w=80, membrane ε_m=4, and protein ε_m=10.

ε_w^{ch}	$\Delta G_{SIP}^{K^+}$ (kT)
40	7.2
80	6.4
200	5.4

Table 2. Distances between K^+ and carbonyl oxygen atoms nearest to it are reported for NMR, GA equilibrated with only water inside (MD_GA), i.e. taken from the MD simulation of the GA channel in the absence of an ion, and GA equilibrated with water and K^+ (MD_GA_K^+) in the course of the MD simulation. To calculate inter-atomic distances, K^+ was placed in the center of the channel for the NMR configuration. For the MD_GA configuration K^+ was placed in the center of the average trajectory configuration after MD simulation. For MD_GA_K^+ configuration K^+ was placed in the center of the NMR configuration and allowed to move in the lateral direction in the course of MD simulation and then the average MD trajectory configuration was used for distance calculations. The changes in K^+-carbonyl oxygen distances between NMR and MD_GA_K^+ (ΔR_{NMR}) configurations and between MD_GA and MD_GA_K^+ (ΔR_{MD}) configurations are also reported. In the first column the backbone carbonyl oxygen atoms to which the distance from K+ ion is measured are referred to by the name and number of the residue in the amino acid sequence of the GA protein.

Name and # of the residue	NMR	MD_GA	MD_GA_K^+	ΔR_{NMR}	ΔR_{MD}
FOR2:O	3.951	4.3	4.25	0.299	-0.05
VAL3:O	4.026	4.014	3.298	-0.728	-0.716
ALA5:O	3.069	3.352	2.87	-0.199	-0.482
ALA7:O	5.142	4.65	4.775	-0.367	0.125
FOR19:O	3.946	3.987	4.031	0.085	0.044
VAL20:O	4.038	4.114	3.126	-0.912	-0.988
ALA22:O	3.087	3.349	2.89	-0.197	-0.459
ALA24:O	5.129	4.718	4.719	-0.41	0.001

Reference List

Allen,T.W., M.Hoyles, S.Kuyucak, and S.H.Chung. 1999. Molecular and Brownian dynamics study of ion selectivity and conductivity in the potassium channel. Chem. Phys. Let. 313:358-365.

Andersen,O.S. and R.E.KoeppeII. 1992. Molecular determinants of channel function. Physiol. Rev. 72:S89-S158.

Antonov,S.M. 2001. Transporters of neurotransmitters: receptive, transport, and channel functions. J. Evol. Biochem. Physiol. 37:328-334.

Aquist,J. 1990. Ion water interaction potentials derived from free-energy perturbation simulations. J. Phys. Chem. 94:8021-8024.

Arsen'ev,A.S., A.L.Lomize, I.L.Barsukov, and V.F.Bystrov. 1986. Gramicidin A transmembrane ion-channel. Three-dimensional structure reconstruction based on NMR spectroscopy and energy refinement. Biol. Membr. 3:1077-1104.

Barcilon,V., D.P.Chen, and R.S.Eisenberg. 1992. Ion flow through narrow membrane channels: Part II. SIAM J. Appl. Math. 53:1405-1425.

Berneche,S. and B.Roux. 2000. Molecular dynamics of the KcsA K+ channel in a bilayer membrane. Biophys. J. 78:2900-2917.

Burykin,A., C.N.Schutz, J.Villá, and A.Warshel. 2002. Simulations of ion current in realistic models of ion channels: the KcsA potassium channel. Proteins: Structure, Function, and Genetics 43:265-280.

Busath,D.D., C.D.Thulin, R.W.Hendershot, L.R.Phillips, P.Maughan, C.D.Cole, N.C.Bingham, S.Morrison, L.C.Baird, R.J.Hendershot, M.Cotten, and T.A.Cross. 1998. Noncontact dipole effects on channel permeation. I. Experiments with (5F-Indole)Trp(13) gramicidin A channels. Biophys. J. 75:2830-2844.

Cardenas,A.E., R.D.Coalson, and M.G.Kurnikova. 2000. Three-dimensional Poisson-Nernst-Planck theory studies: Influence of membrane electrostatics on gramicidin A channel conductance. Biophys. J. 79:80-93.

Chen,D.P. and R.S.Eisenberg. 1993a. Charges, currents, and potentials in ionic channels of one conformation. Biophys. J. 64:1405-1421.

Chen,D.P. and R.S.Eisenberg. 1993b. Flux, coupling, and selectivity in ionic channels of one conformation. Biophys. J. 65:727-746.

Chung,S.H., T.W.Allen, M.Hoyles, and S.Kuyucak. 1999. Permeation of ions across the potassium channel: Brownian dynamics studies. Biophys. J. 77:2517-2533.

Cornell,W.D., P.Cieplak, C.I.Bayly, I.R.Gould, K.M.Merz, D.M.Ferguson, D.C.Spellmeyer, T.Fox, J.W.Caldwell, and P.A.Kollman. 1996. A second generation force field for the simulation of proteins, nucleic acids, and organic molecules. J. Am. Chem. Soc. 118:2309.

Corry,B., T.W.Allen, S.Kuyucak, and S.H.Chung. 2001. Mechanisms of permeation and selectivity in calcium channels. Biophys. J. 80:195-214.

Corry,B., S.Kuyucak, and S.H.Chung. 2000. Tests of continuum theories as models of ion channels. II. Poisson-Nernst-Planck theory versus Brownian dynamics. Biophys. J. 78:2364-2381.

Crozier,P.S., R.L.Rowley, N.B.Holladay, D.Henderson, and D.D.Busath. 2001. Molecular dynamics simulation of continuous current flow through a model biological membrane channel. Phys. Rev. Lett. 86:2467-2470.

Dasent,W.E. 1982. Inorganic energetics. Cambridge University Press, NY

Dieckmann,G.R., J.D.Lear, Q.F.Zhong, M.L.Klein, W.F.DeGrado, and K.A.Sharp. 1999. Exploration of the structural features defining the conduction properties of a synthetic ion channel. Biophys. J. 76:618-630.

Doyle,D.A., J.M.Cabral, R.A.Pfuetzner, u., A., J.M.Gulbis, S.L.Cohen, B.T.Chait, and R.MacKinnon. 1998. The structure of the potassium channel: Molecular basis of K^+ conduction and selectivity. Science 280:69-77.

Eisenberg,R.S. 1999. From structure to function in open ionic channels. J. Membrane Biol. 171:1-24.

Elber,R., D.Rojewska, D.P.Chen, and R.S.Eisenberg. 1995. Sodium in Gramicidin - an example of a permion. Biophys. J. 68:906-924.

Gilson,M.K. and Honig B.H. 1986. The dielectric constant of a folded protein. Biopolymers 25:2097-2119.

Graf,P., M.G.Kurnikova, R.D.Coalson, and A.Nitzan. 2002. Comparison of dynamic Monte-Carlo simulations and dielectric self-energy Poisson Nernst-Plank continuum theory for model ion-channels. manuscript in preparation.

Graf,P., A.Nitzan, M.G.Kurnikova, and R.D.Coalson. 2000. A dynamic lattice Monte Carlo model of ion transport in inhomogeneous dielectric environments: Method and implementation. J. Phys. Chem. B 104:12324-12338.

Hille,B. 1992. Ionic channels of excitable membranes. Sinauer Associates Inc.,

Hille,B., C.M.Armstrong, and R.MacKinnon. 1999. Ion channels: From idea to reality. Nature Med. 5:1105-1109.

Hinsen,K. and B.Roux. 1997. Potential of mean force and reaction rates for proton transfer in acetylacetone. J. Chem. Phys. 106:3567-3577.

Hollerbach,U., D.P.Chen, D.D.Busath, and B.Eisenberg. 2000. Predicting function from structure using the Poisson-Nernst- Planck equations: Sodium current in the gramicidin A channel. Langmuir 16:5509-5514.

Im,W., S.Seefeld, and B.Roux. 2000. A grand canonical Monte Carlo-Brownian dynamics algorithm for simulating ion channels. Biophys. J. 79:788-801.

King,G., F.S.Lee, and A.Warshel. 1991. Microscopic simulations of macroscopic dielectric-constants of solvated proteins. J. Chem. Phys. 95:4366-4377.

Kollman,P.A., I.Massova, C.Reyes, B.Kuhn, S.H.Huo, L.Chong, M.Lee, T.Lee, Y.Duan, W.Wang, O.Donini, P.Cieplak, J.Srinivasan, D.A.Case, and T.E.Cheatham. 2000. Calculating structures and free energies of complex molecules: Combining molecular mechanics and continuum models. Acc. Chem. Res. 33:889-897.

Koprowski,P. and A.Kubalski. 2001. Bacterial ion channels and their eukaryotic homologues. Bioessays 23:1148-1158.

Kurnikova,M.G., R.D.Coalson, P.Graf, and A.Nitzan. 1999. A lattice relaxation algorithm for three-dimensional Poisson- Nernst-Planck theory with application to ion transport through the gramicidin A channel. Biophys. J. 76:642-656.

Kuyucak,S., O.S.Andersen, and S.H.Chung. 2001. Models of permeation in ion channels. Rep. Progr. Phys. 64:1427-1472.

Lide, D.R. 1994. CRC handbook of chemistry and physics. CRC Press.

Lerche,H., K.Jurkat-Rott, and F.Lehmann-Horn. 2001. Ion channels and epilepsy. Amer. J. Med. Genet. 106:146-159.

Luty,B.A., M.E.Davis, and J.A.McCammon. 2002. Solving the finite-difference non-linear Poisson-Boltzmann equation. J. Comp. Chem. 13:1114-1118.

Lynden-Bell,R.M. and J.C.Rasaiah. 1996. Mobility and solvation of ions in channels. J. Chem. Phys. 105:9266-9280.

Mackay,D.H.J., P.H.Berens, K.R.Wilson, and A.T.Hagler. 1984. Structure and dynamics of ion-transport through Gramicidin A. Biophys. J. 46:229-248.

Marban,E. 2002. Cardiac channelopathies. Nature 415:213-218.

Mashl,R.J., Y.Z.Tang, and J.Schnitzer. 2001. Hierarchical approach to predicting permeation in ion channels. Biophys. J. 81:2473-2483.

McQuarrie,D.A. 1976. Statistical Mechanics. Harper Collins Publishers, New York

Nilius,B. and G.Droogmans. 2001. Ion channels and their functional role in vascular endothelium. Physiol. Rev. 81:1415-1459.

Nina,M., S.Berneche, and B.Roux. 2000. Anchoring of a monotopic membrane protein: The binding of prostaglandin H-2 synthase-1 to the surface of a phospholipid bilayer. Eur. Biophys. J. Biophys. Lett. 29:439-454.

Nina,M., W.Im, and B.Roux. 1999. Optimized atomic radii for protein continuum electrostatics solvation forces. Biophys. Chem. 78:89-96.

Nosjean,O., A.Briolay, and B.Roux. 1997. Mammalian GPI proteins: Sorting, membrane residence and functions. BBA-Rev. Biomembranes 1331:153-186.

Partenskii,M.B. and P.C.Jordan. 1992. Theoretical perspectives of ion-channel electrostatics, continuum and microscopic approach. Quat. Rev. Biophysics 91:477.

Roux,B., S.Berneche, and W.Im. 2000. Ion channels, permeation, and electrostatics: Insight into the function of KcsA. Biochemistry 39:13295-13306.

Roux,B. and M.Karplus. 1993. Ion-transport in the gramicidin channel - free-energy of the solvated right-handed dimer in a model membrane. J. Amer. Chem. Soc. 115:3250-3262.

Roux,B. and R.MacKinnon. 1999. The cavity and pore helices the KcsA K+ channel: Electrostatic stabilization of monovalent cations. Science 285:100-102.

Schuss,Z., B.Nadler, and R.S.Eisenberg. 2001. Derivation of Poisson and Nernst-Planck equations in a bath and channel from a molecular model - art. no. 036116. Phys. Rev. E 6403:6116-6123.

Schutz,C.N. and A.Warshel. 2001. What axe the dielectric “constants” of proteins and how to validate electrostatic models? Proteins-Struct. Funct. Genet. 44:400-417.

Sharp.K.A. and Honig B.H. 1990. Electrostatic interactions in macromolecules - theory and applications. Ann. Rev. Biophys. and Biophys. Chem. 19:301-332.

Shobana,S., B.Roux, and O.S.Andersen. 2000. Free energy simulations: Thermodynamic reversibility and variability. J. Phys. Chem. B 104:5179-5190.

Simonson,T. and C.L.Brooks. 1996. Charge screening and the dielectric constant of proteins: Insights from molecular dynamics. J. Am. Chem. Soc. 118:8452-8458.

Smith,G.R. and M.S.P.Sansom. 1999. Effective diffusion coefficients of K+ and Cl- ions in ion channel models. Biophys. Chem. 79:129-151.

Tang,Y.Z., W.Z.Chen, and C.X.Wang. 2000. Molecular dynamics simulations of the gramicidin A- dimyristoylphosphatidylcholine system with an ion in the channel pore region. Eur. Biophys. J. Biophys. Lett. 29:523-534.

Tieleman,D.P., P.C.Biggin, G.R.Smith, and M.S.P.Sansom. 2001. Simulation approaches to ion channel structure-function relationships. Quat. Rev. Biophys. 34:473-561.

Warshel,A. and S.T.Russell. 1984. Calculations of electrostatic interactions in biological-systems and in solutions. Quat. Rev. Biophys. 17:283-422.

Woolf,T.B. and B.Roux. 1997. The binding site of sodium in the gramicidin A channel: Comparison of molecular dynamics with solid-state NMR data. Biophys. J. 72:1930-1945.